

533355

1

Quantitative Laser-Saturated Fluorescence Measurements of Nitric Oxide in
a Heptane Spray Flame

Clayton S. Cooper

Normand M. Laurendeau

Flame Diagnostics Laboratory, School of Mechanical Engineering
Purdue University, West Lafayette, IN 47907-1288

Corresponding author: Clayton S. Cooper
Telephone: (317) 494-5851
Fax: (317) 494-0539
e-mail: ccooper@ecn.purdue.edu



Abstract

We report spatially resolved laser-saturated fluorescence measurements of NO concentration in a pre-heated, lean-direct injection (LDI) spray flame at atmospheric pressure. The spray is produced by a hollow-cone, pressure-atomized nozzle supplied with liquid heptane. NO is excited via the $Q_2(26.5)$ transition of the $\gamma(0,0)$ band. Detection is performed in a 2-nm region centered on the $\gamma(0,1)$ band. Because of the relatively close spectral spacing between the excitation (226 nm) and detection wavelengths (236 nm), the $\gamma(0,1)$ band of NO cannot be isolated from the spectral wings of the Mie scattering signal produced by the spray. To account for the resulting superposition of the fluorescence and scattering signals, a background subtraction method has been developed that utilizes a nearby non-resonant wavelength. Excitation scans have been performed to locate the optimum off-line wavelength. Detection scans have been performed at problematic locations in the flame to determine possible fluorescence interferences from UHCs and PAHs at both the on-line and off-line excitation wavelengths. Quantitative radial NO profiles are presented and analyzed so as to better understand the operation of lean-direct injectors for gas turbine combustors.

Key Words: Laser-Saturated Fluorescence (LSF), Lean-Direct Injection (LDI) , Spray
Flame



Introduction

With the onset of stringent NO_x emissions standards over the last few decades, the attention of the combustion diagnostics community has turned to quantitatively measuring NO concentrations in practical combustion devices. In particular, many researchers have probed liquid-fueled spray flames to better understand the complex flowfields associated with this type of turbulent reactive flow. Structural experimentation has focused on velocity and temperature distributions so as to offer general insight and to aid in the development of numerical models for the flowfield. Lee and Chehrودي (1995), for example, investigated the structure of a swirling, hollow-cone spray flame similar to that occurring in the primary zone of a gas turbine combustor, though at atmospheric pressure. They proposed a mean spray structure based on measurements of the drop size distribution and of mean and rms values of the axial, radial, and tangential drop velocities. Bulzan (1995) investigated a swirl-stabilized, pressure-atomized liquid spray flame by measuring both the gas- and liquid-phase velocity distributions, the drop size distribution, and gas-phase temperature profiles.

Spray flames pose a particular challenge to diagnosticians who seek quantitative measurements of species concentration. Inefficient combustion of the fuel can introduce very large Mie scattering interferences, particularly in the near-field spray region. Because of the large molecular weights of typical hydrocarbon fuels and fuel fragments, fluorescence from unburned hydrocarbons (UHC) and polycyclic aromatic hydrocarbons (PAH) often pose a challenge to selective detection of the spectral signature from the

OPTIONAL FORM 90 (7-90)

FAX TRANSMITTAL

of pages = 3

To <u>DRCK SOTOMAYER</u>	From <u>YOLANDA HILLES</u>
Dept./Agency	Phone #
Fax #	Fax #



species of interest. The most prominent optical methods for *qualitatively* measuring species concentrations in spray flames include UV laser flash photography (UV-LFP) and planar laser-induced fluorescence (PLIF).

Kock *et al.* (1993) utilized UV-LFP to detect spatial distributions of O₂, OH, NO, and fuel for conventional spray flames supplied with either heptane or iso-octane. The burners were designed for oil furnaces and contained an air-swirling baffle plate incorporating various inlets to mix the fuel and air prior to combustion. The excitation wavelengths were 193 nm and 248 nm. Kock *et al.* (1993) encountered interference problems caused by elastically scattered light and fluorescence from hydrocarbons. These problems were overcome by subtracting on- and off-resonance images and by spectral filtering. Calibration was attempted only for NO by simulating exhaust gas conditions in a heated cell and doping various concentrations of NO into the cell while monitoring the signal produced by their experimental apparatus.

Allen *et al.* (1995) obtained qualitative OH distributions in a high-pressure (1-10 atm) spray flame combustor by using PLIF imaging and 283-nm excitation. Heptane, ethanol, and methanol were used as fuels in the combustor. The authors reported hydrocarbon fluorescence interferences which became more problematic at higher pressures. Upschulte *et al.* (1996) obtained qualitative PLIF images of NO, O₂, and fuel vapor by employing excitation wavelengths of 226 nm and 308 nm. Measurements were made for ethanol fuel in the same high-pressure spray flame combustor used by Allen *et al.*



(1995). A broadband interference was again discovered and attributed to hydrocarbon fragments.

Locke *et al.* (1995) utilized PLIF to image OH concentrations in a high-pressure (10-14 atm) combustor supplied with Jet-A fuel (0.59-0.83 kg/s) through lean-direct injection ($\phi=0.41-0.53$) with preheated air (811-866 K). Though this work only assessed the qualitative distribution of OH radicals in the reacting flow, the combustor was designed to simulate actual gas turbine conditions. The authors found that elastically scattered light and PAH fluorescence were not evident in the downstream regions of their LDI-based combustor.

Cessou and Stepowski (1996) recently reported absolute concentration values for OH PLIF images in an atmospheric spray flame produced by a co-axial air-blast injector supplied with methanol. The fluorescence (~ 315 nm) from OH was spectrally discriminated from the elastic scattering (~ 283 nm) produced by the methanol drops, though Raman scattering from the drops required spatial filtering via a novel suppression technique developed by the authors. The OH calibration procedure used an absorption line and its associated linear fluorescence signal at the locations of peak OH concentrations in a reference laminar diffusion flame (Stepowski and Garo, 1985). However, this procedure cannot account for potential quenching effects away from the region of peak [OH] spray flames.



While PLIF and UV-LFP concentration images offer a large amount of data for the chosen flowfields, barriers to quantitative measurements have not been completely overcome by the current technology. Some of these barriers include (1) spatial variations in the electronic quenching rate coefficient, (2) interferences from other species owing to broadband detection, and (3) absorption of the laser sheet as it passes through the control volume. In an effort to make PLIF concentration images quantitative, Partridge *et al.* (1997) have reported a procedure whereby qualitative PLIF images in gaseous flames can be scaled by a small number of laser-saturated fluorescence (LSF) measurements so as to make the images quantitative within the error bars of the more accurate LSF point data.

This study is concerned with quantitative LSF measurements of NO in a swirling liquid-fueled spray flame that incorporates a hollow-cone, pressure-atomized nozzle. The spray flame is based on the lean-direct injection (LDI) configuration, which is of current importance to gas turbine combustion. To our knowledge, these measurements represent the first effort in the combustion diagnostics community to apply the LSF technique to quantitative NO measurements in a turbulent liquid-fueled spray flame. We have focused our measurements to regions of problematic droplet interference, realizing that downstream of the combustion zone and within the hollow cone where droplet interference is negligible, the existing LSF technique should work with little modification.



Experimental Setup

LDI Module

The burner utilized here is based on a lean-direct injection (LDI) design and typifies that used in the primary zone of advanced gas turbine combustors. The stainless steel LDI module (16.5 cm * 3.8 cm dia.) accommodates a fuel tube (6.4 mm dia.) that enters the module co-axially at the bottom (see Fig. 1). For operation at atmospheric pressure, a 60° helical swirler (22.9 mm dia.) is mounted at the top of the fuel delivery tube. The swirler itself is tapped to allow a Delevan 6-mm peanut-nozzle with a 62° spray cone to be directly threaded into the swirler. The nozzle is positioned vertically relative to the converging/diverging orifice (12.7 mm dia. at 40°). The depth of the nozzle below this orifice is adjustable via a slide-through fitting located at the bottom of the module. The air is delivered perpendicular to the module axis and is passed through packed glass beads (~1.5 mm dia.) that fill the module cavity (22.9 mm dia.). The glass beads ensure purely vertical flow of the air entering the air swirler.

The fuel delivery system incorporates a four gallon stainless steel pressure vessel rated at 750 psig. The stored heptane is pressurized with nitrogen and metered via a rotameter flow controller. The air is provided from a building compressor. The air flow is adjusted with a metering valve and monitored with a Hastings model HFM-230 fast-response thermal mass flow meter. Preheating is achieved with two in-line air heaters controlled with voltage regulators. The maximum preheat air temperature is limited by boiling within the fuel tube, which leads to vapor lock in the injector.



The characteristics of general spray flames have been well documented in the literature and provide some applicability to the lean-direct injection. The swirling motion of the air imparted by the helical vanes in this type of burner will affect the combustion efficiency, the temperature distribution, and the species concentrations (Jones and Wilhelmi, 1989). Rink and Lefebvre (1989) have performed a study of the effect of general spray characteristics on NO formation and have shown that the NO_x emissions depend on inlet air temperature, combustion pressure, fuel H/C ratio, and atomization quality. The drop size, which affects combustion efficiency, depends strongly on the axial and radial velocity of the flow, but is apparently independent of the azimuthal component (McDonnell *et al.*, 1992). Lin and Faeth (1996) have demonstrated that entrainment of incipient soot into the flame sheet of laminar diffusion flames inhibits its growth and enhances soot oxidation. A similar effect operates in the intense recirculating flow of the LDI burner.

The special features of LDI combustors have been investigated and are of considerable importance to the design of future gas turbine combustors. Alkabi *et al.* (1988) performed an extensive study of flame stability, NO_x emissions, and combustion efficiency in propane and natural gas fired LDI combustors operated at atmospheric pressure. The authors reported optimum NO_x emissions close to 10 ppm when corrected to 15% excess oxygen. Hayashi (1995) compared the LDI based configuration against a lean premixed-prevaporized (LPP) configuration, both burning kerosene and supplied with pre-heated air at atmospheric pressure. Hayashi (1995)



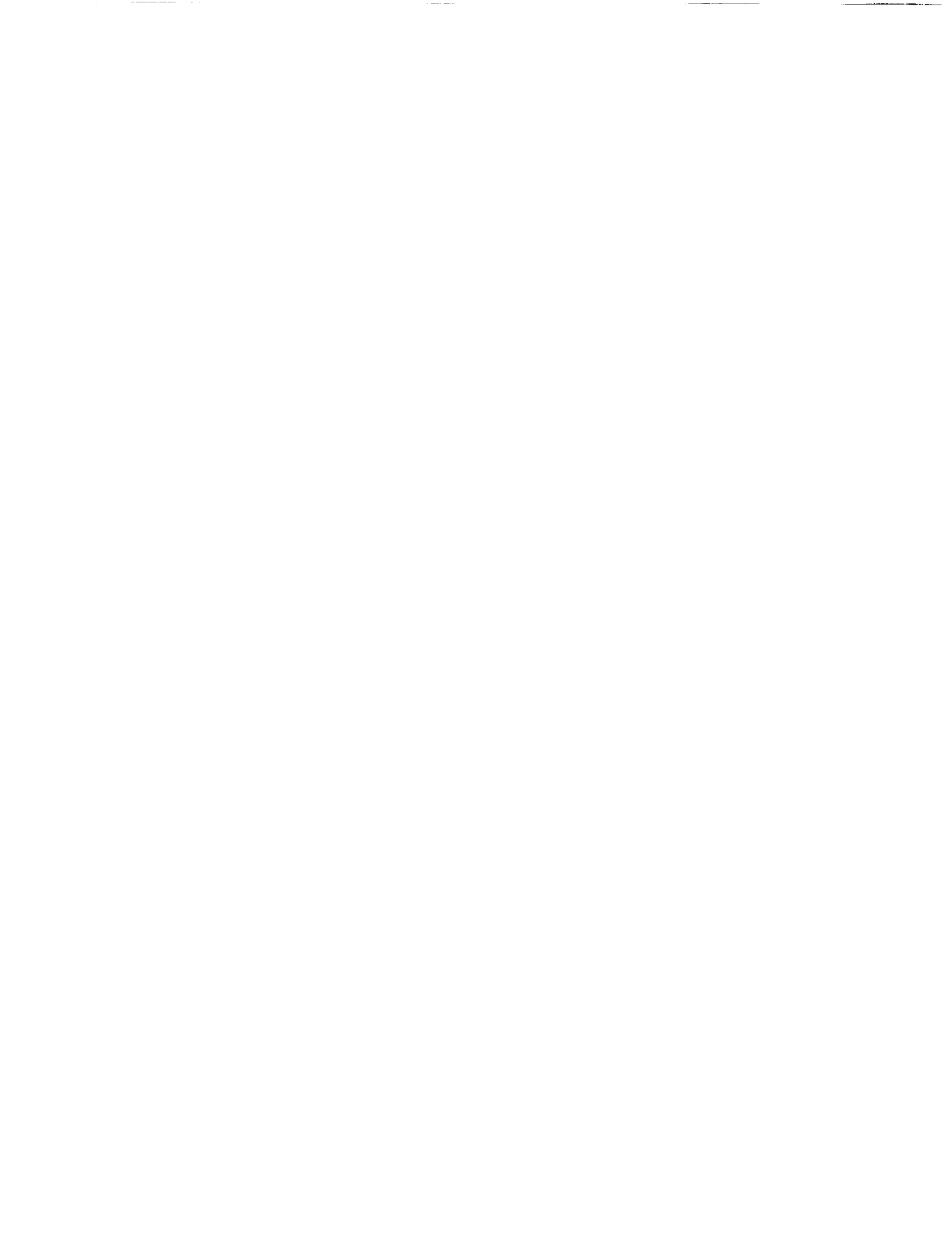
reported higher combustion efficiencies in the direct injection mode and comparable NO_x emissions when the LDI burner was operated leaner than the LPP burner.

LSF Facility

Following the methods described by Reisel *et al.* (1993), excitation of NO is achieved via the Q₂(26.5) line of its $\gamma(0,0)$ band at 225.58 nm. The fundamental (1064 nm) from a Spectra-Physics injection-seeded GCR-4 Nd:YAG laser is frequency doubled (532 nm) and used to pump a tunable PDL-3 dye laser. Pyrromethene 580 dye is employed to generate the PDL fundamental at 572.54 nm (Partridge and Laurendeau, 1994). A WEX-2 Wavelength Extender is used to frequency double the dye laser output to 286.27 nm, followed by frequency mixing with the Nd:YAG fundamental to produce the required 225.58 nm laser beam. The system is equipped with a Fabry-Perot wavelength stabilization system to control PDL drift (Cooper and Laurendeau, 1997). The maximum energy obtained for the mixed beam is ~4 mJ/pulse. The fluorescence from the probe volume (68 μ m wide by 1 mm long) is monitored via a $\frac{3}{4}$ -m monochromator with a Hamamatsu R106-HA PMT specially wired for high temporal resolution. The NO fluorescence signal is averaged over 600 laser shots, while the off-line background is averaged over 300 shots.

Operating conditions

The LDI burner is operated at an equivalence ratio of unity with heptane fuel supplied to the nozzle at 0.3 g/s and air at 4.52 g/s. Though this condition does not yet model lean operation of the LDI module, it was chosen to provide ample NO in the combustion products. The air is



preheated to 475 K to assist in vaporization and mixing of the fuel. The nozzle is located 1.27 mm below the burner throat. At this point, the air has an ~ 48 m/s axial velocity, resulting in a Reynolds number of ~ 17000 . Owing to the intense mixing, the flame is essentially non-sooting and blue, with only an occasional soot tip forming and quickly disappearing (see Fig. 2).

Utility of Excitation/Detection Scheme

Previous work in our laboratory has shown considerable success when performing quantitative NO concentration measurements in a variety of flames produced with gaseous fuels (Reisel and Laurendeau, 1995; Thomsen *et al.*, 1997). Typically, excitation of the $Q_2(26.5)$ line of the $\gamma(0,0)$ band of NO at 225.58 nm is followed by detection of the $\gamma(0,1)$ band with a 2-nm window centered at 235.78 nm. This combination has been selected based on extensive interference and background investigations (Reisel *et al.*, 1993; Partridge *et al.*, 1996). To facilitate use of this excitation/detection scheme in a liquid droplet environment, we must consider the possible effects of Mie scattering interference, fuel and fuel fragment fluorescence, and laser beam absorption.

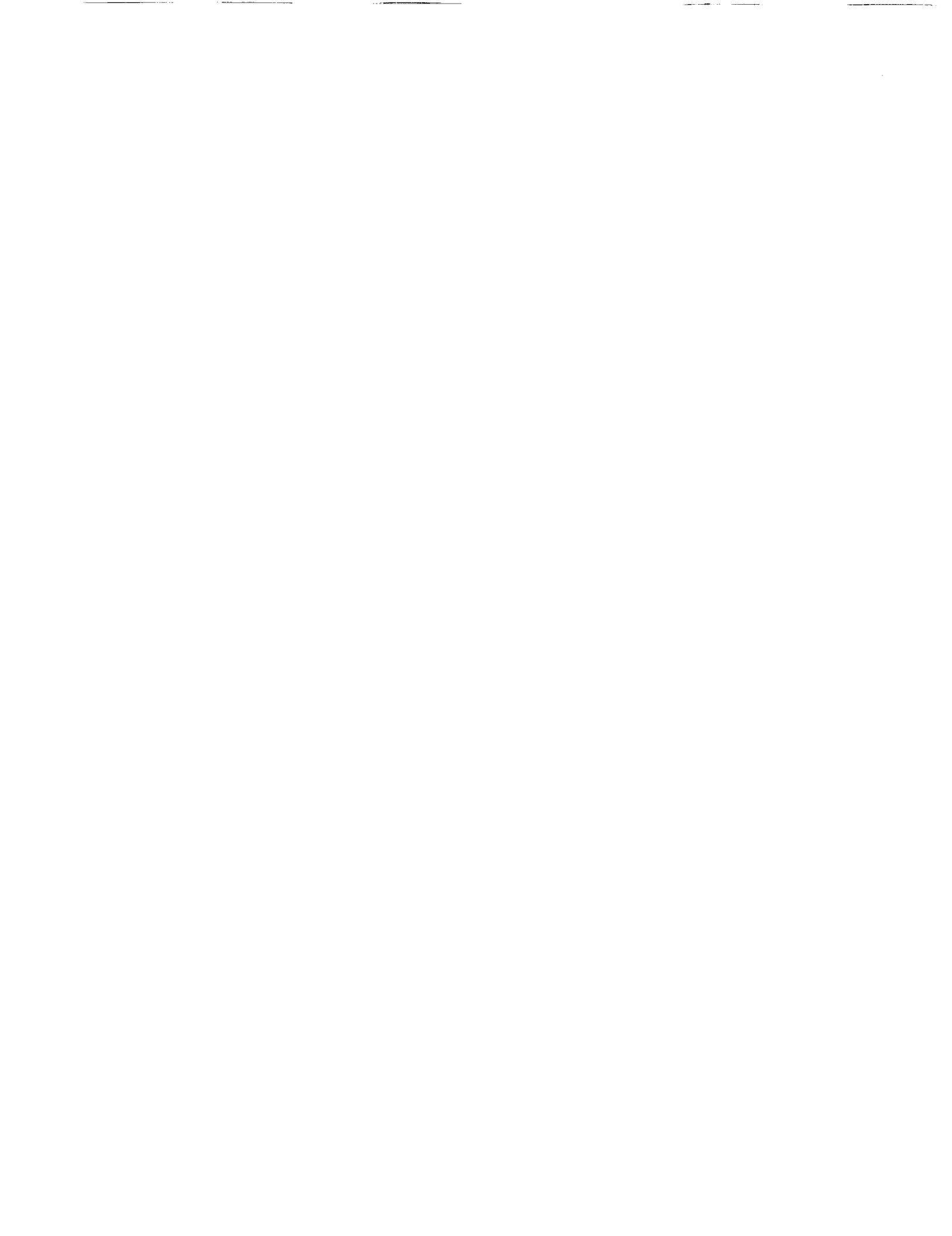
We first assessed the influence of Mie scattering by measuring scattering profiles so as to locate regions of heavy droplet interference. The incident laser wavelength is ~ 226 nm. Scattered light is passed through neutral density filters and collected via a $\frac{3}{4}$ -m monochromator in a 2-nm window centered at ~ 226 nm. Figure 3 indicates the strong Mie scattering that occurs along the spray, especially at lower heights above the burner. As expected, very little interference is present along the centerline. The asymmetry of the radial profiles is a result of the design of the five-vane



helical swirler. Visual observation indicates that the flame is semi-axisymmetric, with five repetitive sliced regions. At greater axial distances, turbulent mixing tends to mesh these regions into an axisymmetric plume.

Excitation and detection scans were next performed in a lean ($\phi=0.8$) $C_2H_6/O_2/N_2/NO$ flame stabilized on a water-cooled McKenna burner (3.76 dilution ratio). The spectral signatures from NO and O_2 have been previously well characterized in such flames (Partridge *et al.*, 1996). Hence, a comparison of spectral scans taken in this standard flame with those obtained in the LDI case will aid in the identification of any interferences resulting from UHC or PAH fluorescence. Figure 4a illustrates a detection scan performed using the McKenna burner with 80 ppm of NO doped into the flame to help define the $\gamma(0,1)$ band structure. Spectral detection was acquired by using a 0.44-nm window with a 0.22-nm spectral spacing between data points.

The first comparative detection scan for the LDI module was obtained at a location where Mie scattering, based on the results shown in Figure 3, exerts a slight influence. Figure 4b indeed demonstrates that at $h=5$ mm, $r=0$ mm, the baseline is not negligible and represents ~15% of the signal in the $\gamma(0,1)$ band. This baseline is a result of the intense Mie scattering and the monochromator instrument function, which produces weak Mie spectral wings that spread ~50 nm in either direction from the excitation wavelength. From this detection scan, no spectral signatures from possible UHCs or PAHs are apparent in the $\gamma(0,1)$ band of NO.



Moving to a location in the flame more heavily plagued by droplet interferences, namely $h=5$ mm, $r=5$ mm (see Fig. 4c), we observe a much larger baseline offset that also tends to grow as the wavelength approaches the excitation wavelength of 225.58 nm. Again, UHCs and PAHs seem to offer no spectral signature in the $\gamma(0,1)$ band. Figures 4b and 4c, however, typify the inherent problem of Mie scattering from droplets. Since we maintain saturation of the $Q_2(26.5)$ line of NO, we are using a relatively high laser power. Unfortunately, the Mie signal scattered from the droplets is linearly proportional to this incident laser power.

Beam absorption at 225.58 nm has also been measured in the LDI flame and has been found to display a maximum absorption of 12% near the burner exit. However, this absorption will not affect NO excitation for saturated conditions. On the other hand, assuming the same degree of absorption at 235.78 nm, a maximum 6% attenuation of the detected fluorescence results, which must be accounted for in the data reduction.

Development of Background Correction Procedure

Quantitative NO measurements in spray flames require a background correction procedure to account for Mie scattering (Fig. 3). Previously, Kock *et al.* (1993) utilized an off-resonance/on-resonance scheme to correct for Mie scattering and also the possible broad-band excitation of UHCs or PAHs for UV-LFP measurements of NO and OH concentrations. An “off-line” excitation wavelength that offers little to no spectral signature from other species in our detection window must be found for this subtraction method to work. An excitation scan obtained in the previously mentioned McKenna burner with 80 ppm doped NO is shown in Figure



5a. In this excitation scan, detection occurs by using a fixed 2-nm window centered at 235.78 nm, i.e., within the $\gamma(0,1)$ band of NO. Figure 5b is a similar excitation scan taken at $h=10$ mm, $r=12$ mm in the LDI flame. Note the overall baseline offset caused by Mie scattering. A candidate off-line location is labeled in both Figures 5a and 5b. No other major species are apparently excited near the $Q_2(26.5)$ transition that would offer substantial interferences to the NO signal.

Previous work by Partridge *et al.* (1996) and Thomsen *et al.* (1997) has shown that an off-line location chosen in the valley between the $P_2(34.5)$ transition of NO and the O_2 interference labeled in Figure 5 constitutes an effective background for representing broadband O_2 interferences at high pressure. Thomsen *et al.* (1997) demonstrated that this off-line location was transportable over a range of lean equivalence ratios and dilution ratios in premixed methane flames. The work reported here addresses the utility of this off-line excitation wavelength with respect to simulation of the Mie background within the NO $\gamma(0,1)$ band without exciting transitions from other species. The off-line location reported in Thomsen *et al.* (1997) is actually shifted to a slightly shorter wavelength than that chosen here. At atmospheric pressure, the spectral difference is negligible and causes no interference problems from major species. However, at higher pressures, the location chosen for this work would lie in the left wing of the O_2 interference shown in Figure 5 (Thomsen *et al.* 1997).

A series of experiments was then undertaken to verify that the off-line excitation wavelength provides a suitable representative of the Mie scattering background. In particular,

these experiments assessed possible NO and hydrocarbon excitations which might occur within the $\gamma(0,1)$ band of NO. First, excitation and detection scans in the previously mentioned McKenna burner were obtained using the off-line location. The results showed some excitation of the $\gamma(0,1)$ band of NO; however, the ensuing NO signal constituted only ~5% of the on-line excitation signal when the monochromator was set to our typical 2-nm detection window. Although this influence is undesirable, a 5% resonant signal can easily be accounted for in the data processing.

To determine if the Mie scattering spectral wings within the $\gamma(0,1)$ band of NO can be modeled via the chosen off-line excitation wavelength, we next obtained broad and narrow detection scans at various locations in the LDI flame with both on-line and off-line excitation. Figure 6a shows typical broad detection scans at a location high enough in the flame where the heptane droplets exert little Mie scattering interference. Figure 6b shows more detailed on- and off-line scans at the same location. In both cases, agreement between the on- and off-line signals is excellent away from the $\gamma(0,1)$ band of NO. Continuing in this vein, broad on- and off-line detection scans were finally taken at a location in the flame plagued by very heavy droplet interference (Fig. 6c). From all of these data, we conclude that the off-line wavelength effectively simulates the Mie scattering spectral profile at locations in the flame where fuel droplets are present.

Despite the above, it is still possible that interferences could exist from UHC and PAH fluorescence in fuel-rich regions of the spray flame. In their PLIF work on OH at high pressure

these experiments assessed possible NO and hydrocarbon excitations which might occur within the $\gamma(0,1)$ band of NO. First, excitation and detection scans in the previously mentioned McKenna burner were obtained using the off-line location. The results showed some excitation of the $\gamma(0,1)$ band of NO; however, the ensuing NO signal constituted only ~5% of the on-line excitation signal when the monochromator was set to our typical 2-nm detection window. Although this influence is undesirable, a 5% resonant signal can easily be accounted for in the data processing.

To determine if the Mie scattering spectral wings within the $\gamma(0,1)$ band of NO can be modeled via the chosen off-line excitation wavelength, we next obtained broad and narrow detection scans at various locations in the LDI flame with both on-line and off-line excitation. Figure 6a shows typical broad detection scans at a location high enough in the flame where the heptane droplets exert little Mie scattering interference. Figure 6b shows more detailed on- and off-line scans at the same location. In both cases, agreement between the on- and off-line signals is excellent away from the $\gamma(0,1)$ band of NO. Continuing in this vein, broad on- and off-line detection scans were finally taken at a location in the flame plagued by very heavy droplet interference (Fig. 6c). From all of these data, we conclude that the off-line wavelength effectively simulates the Mie scattering spectral profile at locations in the flame where fuel droplets are present.

Despite the above, it is still possible that interferences could exist from UHC and PAH fluorescence in fuel-rich regions of the spray flame. In their PLIF work on OH at high pressure



(1-10 atm), Allen *et al.* (1995) discovered an additional broadband fluorescence signal which was excited by their 283-nm laser. They attributed this pressure dependent signal to intermediate hydrocarbon species. Fortunately, the atmospheric flame studied here is a clean blue flame with no steady soot formation. Upshulte *et al.* (1996) also found a broadband interference signal when using 226-nm excitation for PLIF imaging of NO. They simply assigned this interference a nominal 5% of the NO signal at atmospheric pressure. The major aromatic hydrocarbons, i.e., benzene, toluene, and naphthalene, as well as many minor aromatic hydrocarbons, display broad absorption bands with a resolved peak near 250 nm (Beretta *et al.* 1985). Beretta *et al.* (1985) found that the major PAHs within the fuel-rich region of an atmospheric methane diffusion flame generally have maximum emission wavelengths longer than 280 nm. As the excitation wavelength for aromatic hydrocarbons tends toward the UV region, the anti-Stokes component of the emission band becomes almost negligible. In particular, Petarca and Marconi (1989) did not record an anti-Stokes component of PAH fluorescence in the pyrolysis region of an *n*-heptane diffusion flame when using UV excitation wavelengths. For the 225.58-nm excitation wavelength used in our experiments, fluorescence emission should be negligible at the detection wavelength of 235.78 nm. On the other hand, any fluorescence from large molecules such as UHCs or PAHs that might exist in fuel-rich regions would invariably exhibit broad absorption and fluorescence signatures and thus would be superimposed onto the more prominent Mie scattering signal. The off-line excitation signal for these types of molecules would be comparable to that for on-line excitation and so would be subtracted out in the background correction process.



A more instructive method by which to validate the utility of the chosen off-line excitation wavelength is to compare radial profiles for the off-line and Mie scattering signals. In Figure 7, the off-line signal has been monitored by using the same procedure as used for the NO measurements, namely a 2-nm window centered at 235.78 nm. The corresponding Mie signal has been monitored with a 2-nm window centered near the laser wavelength of 225.58 nm. For comparative purposes, each radial off-line signal profile has been scaled to the corresponding maximum radial Mie signal. Since the off-line/Mie scattering correlation should hold at locations in the flame where the liquid droplets exert a negligible influence, any additional interference would tend to disrupt the correlation in fuel-rich zones, i.e., in those regions where heavy droplet interference is present. However, such a result is not evident from Figure 7. In particular, a good correlation between the off-line and Mie scattering signal is obtained, even in the fuel-rich zones of the flame.

Background Subtraction Methodology

By using the LSF technique, we avoid laser power corrections to and quenching of the NO fluorescence signal. However, Mie scattering is linearly proportional to the incident laser irradiance. To verify that the off-line signal scales linearly with laser power, Figure 8 displays the results obtained when monitoring the $\gamma(0,1)$ band of NO while varying the incident laser power at the off-line excitation wavelength (225.54 nm). The linearity of the data is consistent with our supposition that the off-line signal represents the Mie spectral wings. However, linear fluorescence from other species could be included in the off-line signal.



In general, we expect that the on-line signal measured by the photo-multiplier tube (PMT) consists of NO fluorescence ($S_{NO, On-line}$) and Mie scattering ($S_{Mie, On-line}$), i.e.,

$$S_{PMT, On-line} = S_{NO, On-line} + S_{Mie, On-line} \quad (1)$$

To reduce the PMT signal to the NO fraction of the collected radiation, we tune the PDL to the off-line wavelength and collect the resulting signal. Correcting for variations in laser power, P , between the on-line and off-line measurements, the on-line Mie signal will be

$$S_{Mie, On-line} = \frac{S_{Mie, Off-line}}{P_{Off-line}} \cdot P_{On-line} \quad (2)$$

Both S and P are also corrected to account for the electronic background of the boxcar data acquisition system. As discussed previously, the final NO signal must account for the absorption (and scattering) of fluorescence by the liquid droplet environment. The fraction of signal absorbed is defined by $x_{absorption}$. In addition, the off-line signal contains a resonant excitation of the $\gamma(0,1)$ band of NO. This fraction is defined by $x_{resonant}$. Finally, the NO signal can be computed as follows:

$$S_{NO, On-line} = \frac{S_{PMT, On-line}}{1 - x_{absorption}} - S_{Mie, Off-line} \cdot \frac{P_{On-line}}{P_{Off-line}} \cdot \frac{1 - x_{resonant}}{1 - x_{absorption}} \quad (3)$$

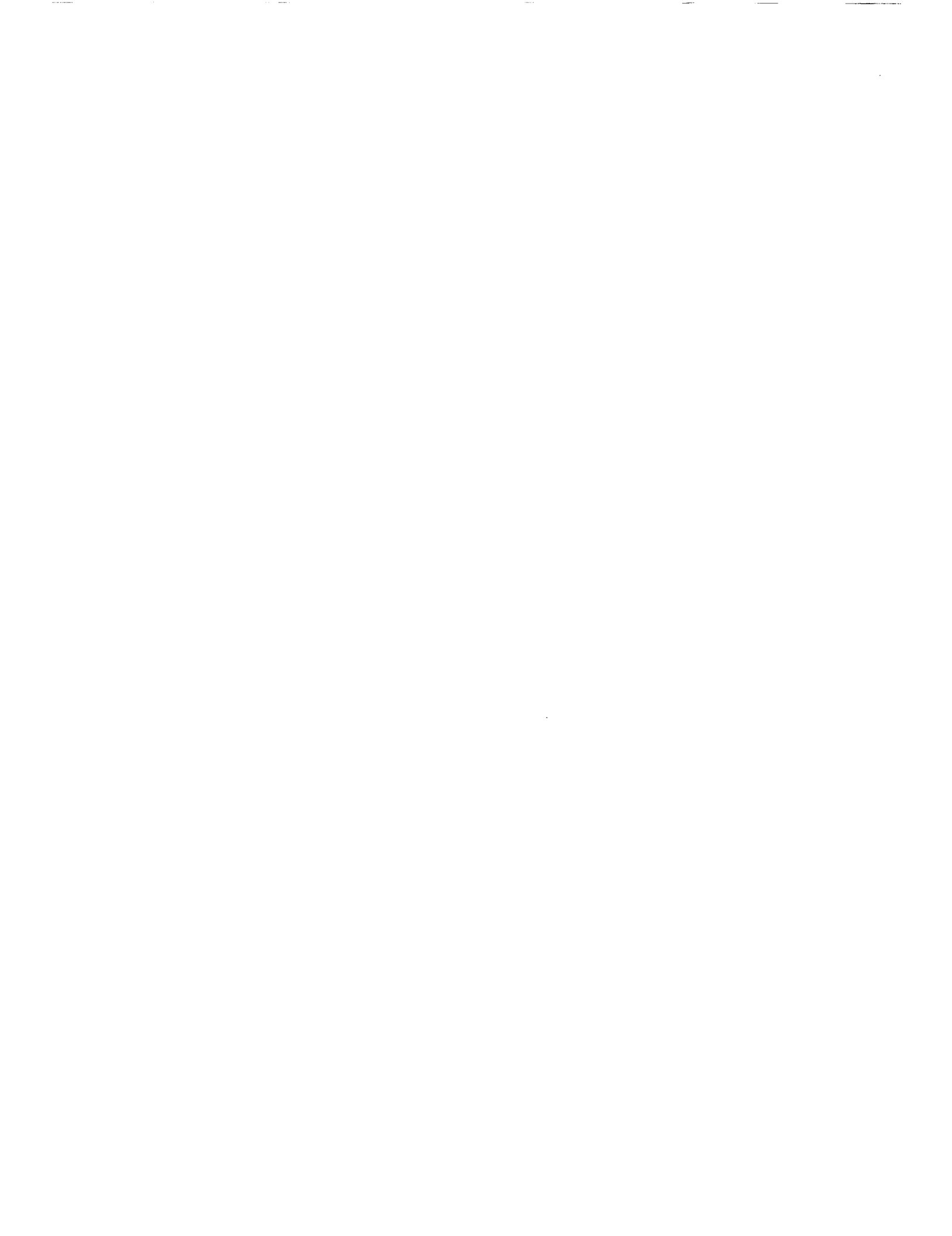


The absorption fraction varies with axial height. For our worst case conditions, $x_{absorption} \cong 6\%$. The resonant excitation fraction is constant at $x_{resonant} \cong 5\%$. The NO signal is converted to an absolute concentration via a calibration performed in a $\phi=0.8$ $C_2H_6/O_2/N_2/NO$ flame stabilized on a water-cooled Mckenna burner. Varying amounts of NO were doped into the calibration flame and the resulting PMT signal recorded to produce a linear calibration plot.

NO Concentration Profiles

Given the verification of an off-line wavelength that effectively models the Mie scattering spectral wings within the region of the spectrum occupied by the $\gamma(0,1)$ band of NO, we may now present our measured radial NO concentration profiles (Fig. 9). The most striking observation from a comparison of these [NO] profiles with the Mie scattering profiles discussed earlier is the difference in shape. While the Mie scattering profiles show a non-symmetric, double-peak structure owing to the conical spray cone and the air swirl, the NO profiles are distributed almost symmetrically about the centerline. This symmetry is due to the intense recirculation of the combustion products and oxidizer into the center of the flame structure. Similarly, as the axial distance from the burner is increased from 2.5 to 10 mm, the NO concentration increases and then flattens at 10-20 mm because of the strong mixing in the recirculation zone (Lee and Chehroudi, 1995). Past this axial distance, the peak NO concentration decreases owing to entrainment of outside air.

The NO concentration on the negative coordinate side of Figure 9 is slightly lower than that on the positive coordinate side. This lower concentration corresponds to the larger Mie



signal as measured in Figure 3. The prominent dips in the [NO] profiles on the negative coordinate axis correspond to regions near the liquid droplets. Finally, the error bars shown on the profiles describe the accuracy of the centerline point and the two radial points that correspond to the maximum Mie signal shown in Figure 3. The relative errors (95% confidence limit) associated with the concentration measurements generally range between 20% and 35%. In comparison, previous LSF work in gaseous flames yields typical relative errors of 15-20% (Reisel *et al.*, 1993).

To gauge the ppm values of NO within this flame, we measured the centerline temperature at ~20 mm above the burner with a thermocouple. The resulting temperature, uncorrected for radiation, is ~1200 K. Given the concentration measured in Figure 9, this temperature corresponds to ~55 ppm of NO. Recall that the overall equivalence ratio for this study is unity. Were the LDI burner operated at lower equivalence ratios, the NO concentration levels would be considerably lower.

Conclusions

Quantitative LSF measurements of NO concentration have been obtained in an LDI burner fueled with liquid heptane at atmospheric pressure. The current technology for LSF measurements of NO has been extended to a liquid droplet environment by developing a correction procedure for Mie scattering. Employing an excitation wavelength resonant with the NO Q₂(26.5) line, the NO fluorescence signal and Mie scattering signal are detected within a 2-



nm window centered on the NO $\gamma(0,1)$ band. The inherent Mie scattering portion is separately determined by employing an excitation wavelength shifted from the NO transition. A subtraction method is then implemented to reduce these signals to quantitative NO concentrations. Experiments have shown that possible fluorescence interferences from UHCs or PAHs are apparently negligible within the $\gamma(0,1)$ detection window. The measured NO profiles in the LDI burner are essentially symmetric, as expected from the intense recirculation pattern characteristic of LDI-based flames.

Acknowledgments

This research was funded by the National Aeronautics and Space Administration (Lewis Research Center) through General Electric Aircraft Engines, Cincinnati, OH. We thank our project technical monitors, Mr. Chi Lee of NASA and Mr. Claude Chauvette of General Electric. The design of the LDI module was aided by Phil Lee of Fuel Systems Textron and Mark Durbin of General Electric. Bob Tacina of NASA provided the helical swirlers. C.S. Cooper acknowledges support by a National Defense Science and Engineering Graduate Fellowship.



REFERENCES

- Alkabie, H.S., Andrews, G.E. and Ahmad, N.T. (1988). Lean Low NO_x Primary Zones Using Radial Swirlers. ASME Paper No. 88-GT-245, International Gas Turbine and Aeroengine Congress and Exposition, June 1988.
- Allen, M.G., McManus, K.R., Sonnenfroh, D.M. and Paul, P.H. (1995). Planar Laser-Induced-Fluorescence Imaging Measurements of OH and Hydrocarbon Fuel Fragments in High-Pressure Spray Flame Combustion. *Applied Optics* **34**, 6287-6300.
- Beretta, F., Cincotti, V., D'Alessio A. and Menna P. (1985). Ultraviolet and Visible Fluorescence in the Fuel Pyrolysis Regions of Gaseous Diffusion Flames. *Combust. and Flame* **61**, 211-218.
- Bulzan, D. (1995). Structure of a Swirl-Stabilized Combusting Spray. *J. Propul. Power* **11**, 1093-1102.
- Cessou, A. and Stepowski D. (1996). Planar Laser Induced Fluorescence Measurements of [OH] in the Stabilization Stage of a Spray Jet Flame. *Combust. Sci. and Tech.* **118**, 361-381.
- Cooper, C.S. and Laurendeau, N.M. (1997). Effect of Pulsed Dye Laser Wavelength Stabilization on Spectral Overlap in Atmospheric NO Fluorescence Studies. Submitted for publication to *Applied Optics*.



- Hayashi, S. (1995). Compatibility Between Low-NO_x Emissions and High-Combustion Efficiency by Lean Direct Injection Combustion. ASME Paper No. 95-GT-276. International Gas Turbine and Aeroengine Congress and Exposition, June 1995.
- Jones, W.P. and Wilhelmi J. (1989). Velocity, Temperature, and Composition Measurements in a Confined Swirl Driven Recirculating Flow. *Combust. Sci. and Tech.* **63**, 13-31.
- Kock, A. Chrysostomou, A., Andresen, P. and Bornsheuer, W. (1993). Multi-Species Detection in Spray Flames with Tunable Excimer Lasers. *J. Appl. Phys. B* **56**, 165-176.
- Lee, K. and Chehroudi, B. (1995). Structure of a Swirl-Stabilized Spray Flame Relevant to Gas Turbine and Furnaces. *J. Propul. Power* **11**, 1110-1117.
- Lin, K.C. and Faeth, G.M. (1996). Hydrodynamic Suppression of Soot Emissions in Laminar Diffusion Flames. *J. Propul. Power* **12**, 10-16.
- Locke, R.J., Hicks, Y.R., Anderson, R.C., Ockunzzi, K.A. and North, G.L. (1995). Two-Dimensional Imaging of OH in a Lean Burning High Pressure Combustor. AIAA Paper No. 95-0173, AIAA 33rd Aerospace Sciences Meeting & Exhibit, January 1995.



- McDonnel, V.G., Adachi, M. and Samuelsen, G.S. (1992). Structure of Reacting and Non-Reacting Swirling Air-Assisted Sprays. *Combust. Sci. and Tech.* **82**, 225-248.
- Partridge, W.P. and Laurendeau, N.M. (1994). Performance of Pyrromethene 580 and 597 in a Commercial Nd:YAG-Pumped Dye-Laser System. *Optics Letters* **19**, 1630-1632.
- Partridge, W.P., Klassen, M.S. Jr., Thomsen, D.D. and Laurendeau, N.M. (1996). Experimental Assessment of O₂ Interferences on Laser-Induced Fluorescence Measurements of NO in High-Pressure, Lean Premixed Flames by use of Narrow-Band and Broad-Band Detection. *Applied Optics* **34**, 4890-4904.
- Partridge, W.P. and Laurendeau N.M. (1997). Development and Application of Experimentally Based Correction Procedures for Planar Laser-Induced Fluorescence Measurements of Species Concentration. Submitted for publication to *Applied Optics*.
- Petarca, L. and Marconi F. (1989). Fluorescence Spectra and Polycyclic Aromatic Species in a N-Heptane Diffusion Flame. *Combust. Flame.* **78**, 308-325.
- Reisel, J.R., Carter, C.D. and Laurendeau, N.M. (1993). Laser-Saturated Fluorescence Measurements of Nitric Oxide in Laminar, Flat, C₂H₆/O₂/N₂ Flames at Atmospheric Pressure. *Combust. Sci. and Tech.* **91**, 271-295.



- Reisel, J.R. and Laurendeau, N.M. (1995). Quantitative LIF Measurements and Modeling of Nitric Oxide in High Pressure $C_2H_4/O_2/N_2$ Flames. *Combust. Flame*. **101**, 141-152.
- Rink, K.K. and Lefebvre, A.H. (1989). The Influences of Fuel Composition and Spray Characteristics on Nitric Oxide Formation. *Combust. Sci. and Tech.*, **68**, 1-14.
- Stepowski, D. and Garo, A. (1985). Local Absolute OH Measurements in a Diffusion Flame by Laser Induced Fluorescence. *Applied Optics* **24**, 2478-2480.
- Thomsen, D.D., Kuligowski, F.F. and Laurendeau, N.M. (1997). Background Corrections for Laser-Induced Fluorescence Measurements of NO in Lean, High-Pressure, Premixed Methane Flames. Accepted for publication in *Applied Optics*.
- Upschulte, B.L., Allen, M.G. and McManus K.R. (1996). Fluorescence Imaging of NO, O₂, and Fuel Vapor in a High Pressure Spray Flame Combustor. Paper No. 96-0536, AIAA 34th Aerospace Science Meeting & Exhibit, January 1996.

Figure Captions:

- Figure 1:** Cutaway drawing of LDI burner. The burner is constructed of stainless steel with a fuel tube entering co-axially at the bottom of the burner and air entering perpendicular to the axis. The air is passed through packed glass beads to attain purely vertical flow and then directed through a helical-vane swirler. Fuel is injected immediately after the swirler by utilizing a small pressure-atomized nozzle.
- Figure 2:** Photograph of the flame studied for this work. The non-sooting blue flame is achieved with the following operating parameters of the LDI burner: (1) $\dot{m}_{fuel} = 0.3$ g/s, (2) $\phi=1$, (3) $d_{nozzle}=1.27$ mm, and (4) $T_{air\ preheat}=475$ K.
- Figure 3:** Mie scattering radial profiles for LDI flame at four axial heights. Excitation and detection were performed at 225.58 nm. The asymmetry is a result of the design of the five-vane helical air swirler. The flame is semi-axisymmetric with five repetitive sliced regions.
- Figure 4:** Detection scans performed in (a) McKenna burner ($\phi=0.8$, 3.76 dilution ratio) doped with 80 ppm NO, (b) LDI burner at $h=5$ mm, $r=0$ mm, and (c) LDI burner at $h=5$ mm, $r=5$ mm. Excitation is achieved via the $Q_2(26.5)$ line in the $\gamma(0,0)$ band of NO. These scans show no evidence of possible UHC or PAH fluorescence interferences.



- Figure 5:** Excitation scans in (a) McKenna burner ($\phi=0.8$, 3.76 dilution ratio) doped with 80 ppm NO, (b) LDI burner at $h=10$ mm, $r=12$ mm. The NO $Q_2(26.5)$ and the off-line excitation wavelengths are labeled.
- Figure 6:** Detection scans in the LDI module for on- and off-line excitation to assess simulation of the Mie background when using the off-line wavelength. (A) Broad-band detection scan at $h=10$ mm $r=12$ mm. (B) Narrow-band detection scan at $h=10$ mm, $r=12$ mm. (C) Broad-band detection scan at $h=5$ mm, $r=7$ mm.
- Figure 7:** Comparison of radial off-line excitation and Mie scattering profiles. The off-line signal is monitored with the typical detection window used for NO measurements, namely a 2-nm window centered at 235.78 nm. The Mie scattering signal is monitored with a 2-nm window centered around the laser wavelength of 225.58 nm. Each radial off-line signal profile has been scaled to the corresponding maximum radial Mie signal for comparative purposes. The excellent correlation indicates that the off-line signal chosen effectively simulates the Mie background signal.
- Figure 8:** Linear scaling of the off-line signal with laser power. The linear correlation yields confidence that the off-line signal represents the Mie scattering.

Figure 9: Radial NO concentration profiles in the LDI burner ($\dot{m}_{\text{fuel}} = 0.3 \text{ g/s}$, $\phi=1$, $d_{\text{nozzle}}=1.27 \text{ mm}$, $T_{\text{air}}=475 \text{ K}$) at four axial heights.

